Title
Chemiluminescent Probes for Activity-Based Sensing of Formaldehyde Released from Folate Degradation in Living Mice.

Journal
Angewandte Chemie (International ed. in English), 57(25)

ISSN
1433-7851

Authors
Bruemmer, Kevin J
Green, Ori
Su, Timothy A
et al.

Publication Date
2018-06-01

DOI
10.1002/anie.201802143

Peer reviewed

Biosensors

International Edition: DOI: 10.1002/anie.201802143
German Edition: DOI: 10.1002/ange.201802143

Chemiluminescent Probes for Activity-Based Sensing of Formaldehyde Released from Folate Degradation in Living Mice

Kevin J. Bruemmer[+], Ori Green[+], Timothy A. Su[+], Doron Shabat, and Christopher J. Chang**

Abstract: *Formaldehyde (FA) is a common environmental toxin that is also produced naturally in the body through a wide range of metabolic and epigenetic processes, motivating the development of new technologies to monitor this reactive carbonyl species (RCS) in living systems. Herein, we report a pair of first-generation chemiluminescent probes for selective formaldehyde detection. Caging phenoxy-dioxetane scaffolds bearing different electron-withdrawing groups with a general 2-aza-Cope reactive formaldehyde trigger provides chemiluminescent formaldehyde probes 540 and 700 (**CFAP540** and **CFAP700**) for visible and near-IR detection of FA in living cells and mice, respectively. In particular, **CFAP700** is capable of visualizing FA release derived from endogenous folate metabolism, providing a starting point for the use of CFAPs and related chemical tools to probe FA physiology and pathology, as well as for the development of a broader palette of chemiluminescent activity-based sensing (ABS) probes that can be employed from in vitro biochemical to cell to animal models.*

Formaldehyde (FA) is a reactive carbonyl species (RCS) most commonly associated with being an external environmental pollutant, but it is also produced internally through a diverse array of biological processes.[1,2] This major one-carbon unit lies at the nexus of metabolism and epigenetics, participating in the synthesis of key biological molecules, including purines, amino acids, and neurotransmitters,[3–5] as well as in the methylation status of a variety of nucleic acid, protein, and small-molecule metabolites.[6–10]

The small and transient nature of FA has motivated growing interest in developing new activity-based sensing (ABS) methods[11–14] for selective FA detection,[15,16] including aza-Cope,[17–24] aminal,[25,26] and formimine[27–32] reaction-based approaches. Indeed, recent progress in developing fluorescent probes for FA detection in cells has elucidated more sophisticated biological roles for FA as both an exogenous toxin and an endogenous signaling molecule. Included is the discovery that FA is endogenously produced in the folate cycle through specific intermediates like tetrahydrofolate and 5,10-methylenetetrahydrofolate, but not others like 5-methyltetrahydrofolate,[8] opening new doors to investigate the intriguing yet complex relationships between FA, methylation status, and carcinogenesis. Despite these advances in fluorescent FA detection, FA imaging in living mammals is limited to an aza-Cope-based PET tracer,[19] which requires specialized equipment to implement. As such, we sought to develop a single, general platform for FA-selective ABS that would be applicable across a broader spectrum of biological models from in vitro biochemical to cell to in vivo animal systems. To this end, we turned our attention to chemiluminescent imaging, which offers an attractive approach in that it does not require external light irradiation, resulting in minimal background signal.[33–37] Herein, we report first-generation chemiluminescent probes capable of visualizing changes in FA from in vitro to in vivo mouse models, offering a versatile approach for ABS of this central one-carbon molecule.

Our design relies upon a class of luminophores based on Schaap's dioxetane,[38,39] which has been exploited to create chemiluminescent probes for analytes spanning reactive oxygen/sulfur species[40–44] and enzyme activity.[42,45,46] Recent work from one of our labs has shown that introducing electron-withdrawing groups at the *ortho* position of the phenol can result in a 1000-fold increase in chemiluminescence quantum efficiency and the ability to tune emission profiles,[42] particularly to the near-IR region to enable better tissue penetration for in vivo imaging.[47] Based on this scaffold, we created a set of chemiluminescent FA probes by caging this phenol with a 2-aza-Cope FA-reactive trigger (Scheme 1).[20] Chemiluminescent formaldehyde probes 540 and 700 (**CFAP540** and **CFAP700**) feature visible and near-IR emission profiles designed for in vitro cell and in vivo animal applications, respectively (see the Supporting Information for synthetic details). Reaction of FA at the homoallylamine, followed by immolation of the two-carbon linker through a β-elimination, yields the free phenoxy-dioxetane that subsequently decomposes through chemiexcitation to produce a photon.

With these CFAP reagents in hand, we first evaluated their chemiluminescent responses to FA (Figure 1) by adding a large excess of FA (10 mM) and measuring the light emission

[*] K. J. Bruemmer,[+] Dr. T. A. Su,[+] Prof. C. J. Chang
Department of Chemistry, University of California, Berkeley
Berkeley, CA 94720 (USA)
E-mail: chrischang@berkeley.edu
O. Green,[+] Prof. D. Shabat
School of Chemistry, Faculty of Exact Sciences, Tel Aviv University
Tel Aviv 69978 (Israel)
E-mail: chdoron@post.tau.ac.il
Prof. C. J. Chang
Department of Molecular and Cell Biology, University of California, Berkeley
Berkeley, CA 94720 (USA)
and
Howard Hughes Medical Institute
Chevy Chase, MD 20815 (USA)
[+] These authors contributed equally to this work.
Supporting information and the ORCID identification number(s) for the author(s) of this article can be found under: https://doi.org/10.1002/anie.201802143.

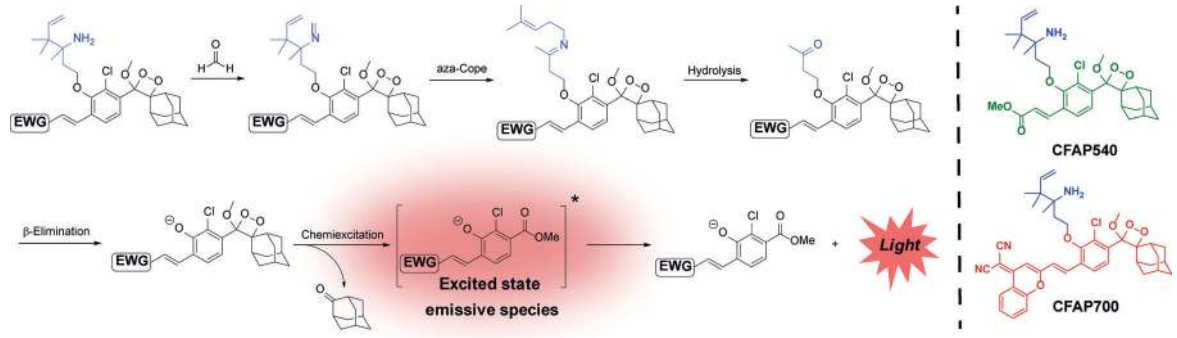

Scheme 1. Reaction pathway of the 2-aza-Cope trigger followed by chemiexcitation of CFAP probes allows for the detection of formaldehyde. Chemical structures of **CFAP540** and **CFAP700**. (EWG = Electron-withdrawing group)

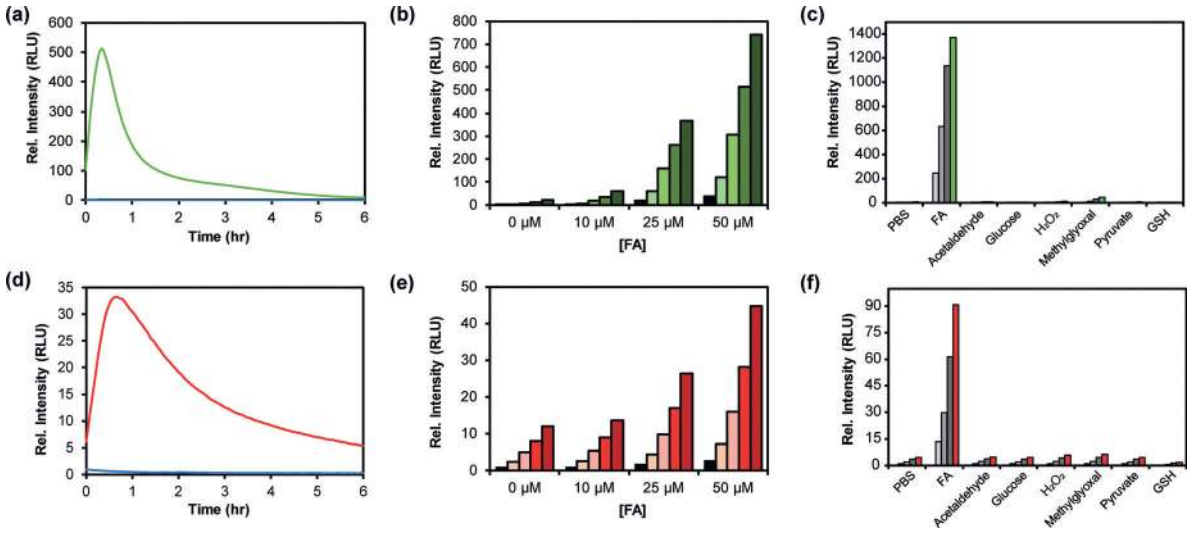

Figure 1. Chemiluminescence kinetic profiles of 10 μM a) **CFAP540** or d) **CFAP700** to 0 μM FA (blue trace) and 10 mM FA (green or red trace) in PBS (10 mM, pH 7.4, 10% FBS) at 37°C. Chemiluminescence responses of 10 μM b) **CFAP540** or e) **CFAP700** to 0, 10, 25, and 50 μM FA. Data were acquired in DMEM growing media at 37°C. Bars represent time points taken at 0 (black), 30, 60, 120 and 240 min (green or red) after addition of FA. Chemiluminescence responses of 10 μM c) **CFAP540** or f) **CFAP700** to RCS or relevant biological analyte. Bars represent emission intensity responses to 100 μM analyte for 0 (lightest gray), 30 (light gray), 60 (gray), 90 (dark gray), and 120 (colored) min.

over several hours. The probes displayed a robust response to FA, with maximum light emission obtained within the first 60 min. **CFAP540** exhibits a maximum intensity increase of 500-fold compared to baseline (Figure 1a) with **CFAP700** showing a 33-fold intensity increase (Figure 1d). The lower observed turn-on response for **CFAP700** is likely due to minor off-pathway uncaging in buffered solution (Supporting Information, Figure S5). To test responses to physiological concentrations of FA, the probes were exposed to 0, 10, 25, and 50 μM FA. Under these conditions, both **CFAP540** and **CFAP700** could detect 25–50 μM levels of FA, while **CFAP540** could detect 10 μM changes in FA owing to its superior signal-to-noise response. Owing to their shared aza-Cope trigger, the CFAP reagents are highly selective for FA, with minimal emission observed upon reaction with other biologically relevant aldehydes and molecules (Figure 1c,f).

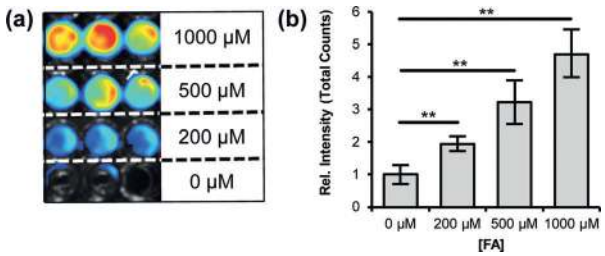

Figure 2. HEK293 cells were treated with **CFAP540** (10 μM, 0.1% DMSO) and incubated for 30 min in growth medium. Growth medium was removed and cells were washed thrice with PBS (pH 7.4) Then, cells were treated with 0, 200, 500, and 1000 μM FA and the chemiluminescence signal was collected for 90 min. a) Representative chemiluminescence cell images in triplicate. b) Quantification of total light emitted from the cells after 90 min. Error bars = SEM ($n = 6$), and statistical analyses were performed with a two-tailed Student's t test where $^{**}P \leq 0.01$.

We next determined the ability of the CFAP platform to detect FA in living cells (Figure 2). HEK293 cells were first incubated with 10 μM **CFAP540** for 30 min in Dulbecco's modified Eagle medium (DMEM), then washed three times with phosphate-buffered saline (PBS) to remove excess probe. **CFAP700**, which lacks the esterase-sensitive methyl ester substituent found in **CFAP540**, is not cell-trappable under these repeated washing conditions and was not employed for cellular FA detection. Chemiluminescent signal was then measured for 90 min after exogenous addition of 0, 200, 500, or 1000 μM FA and showed a dose-dependent increase for **CFAP540**. Flow cytometry experiments confirm that the cells remain viable throughout the course of the experiment (Supporting Information, Figure S8).

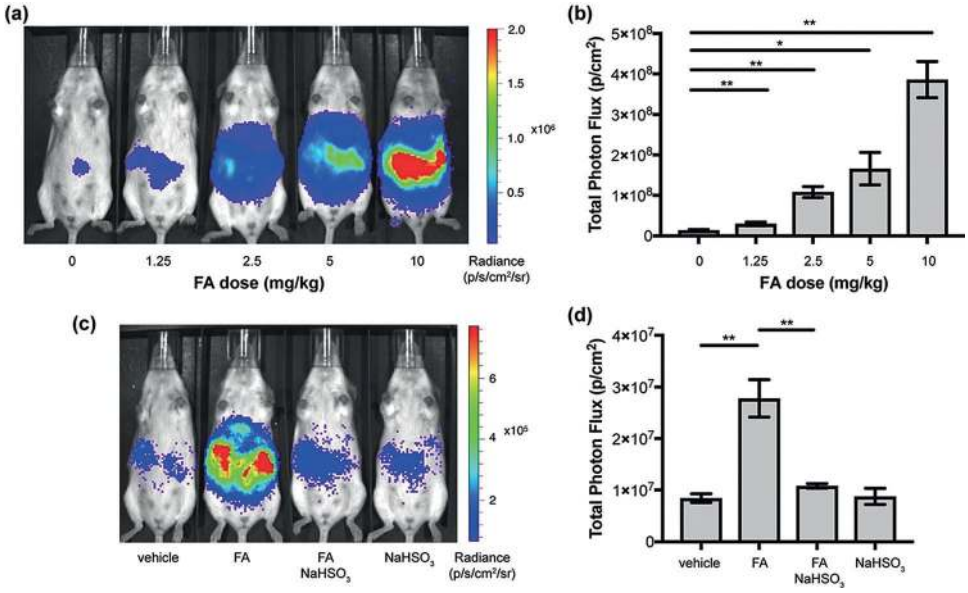

Figure 3. Chemiluminescent imaging of **CFAP700** in response to exogenous FA and FA scavenger treatment. FVB-luc+ mice were injected (i.p.) with FA in water, then injected with 100 μM **CFAP700** (100 μL, 1% DMSO, 1% BSA in PBS). The mice were imaged every 2.5 min from 0–25 min. a) Representative images of FVB-luc+ mice injected with **CFAP700** and varying doses of FA. b) Total photon flux, integrated from 0–25 min post injection with region of interest over the intraperitoneal cavity. Error bars = SEM ($n = 3$). c) FVB-luc+ mice were injected (i.p.) with aqueous FA (2.5 mpk) or water, then aq. sodium bisulfite (25 mpk) or water, then 100 μM **CFAP700** (100 μL). Representative images of FVB-luc+ mice injected with **CFAP700**, FA, and/or sodium bisulfite. d) Total photon flux, integrated from 0–25 min post injection. Error bars = SEM ($n = 3$–4). b,d) Statistical analyses were performed with a two-tailed Student's t test where $^*P \leq 0.05$,$^{**}P \leq 0.01$.

We then evaluated the CFAP platform for in vivo FA imaging in mouse models and utilized the red-shifted emission profile of **CFAP700** for deeper tissue penetration. We first sought to establish that **CFAP700** can detect exogenous FA addition in living animals in a dose-dependent manner. Anesthetized FVB-luc$^+$ mice received intraperitoneal (i.p.) injections of 0, 1.25, 2.5, 5, or 10 mg kg^{-1} FA in water; all doses are well below the LD_{50} range for FA reported for rodents.[48] The mice received subsequent i.p. injections of 100 μM **CFAP700**. Five minutes after injection, the mice were imaged with an IVIS luminescence instrument every 2.5 min over a 25-minute period. Figure 3a provides representative images of five mice injected with increasing amounts of FA. We observed a 1.8-fold increase at the lowest administered dose of 1.25 mpk, and a 28-fold increase at the highest administered dose (10 mpk), highlighting the significant dynamic range of the **CFAP700** probe for in vivo FA detection in these mouse models.

To support these results, we injected (i.p.) mice with either 2.5 mpk FA or water vehicle, then injected either 25 mpk sodium bisulfite as a FA scavenger or water vehicle, then injected 100 μM **CFAP700**. Mice that were injected with FA and sodium bisulfite showed no statistically significant difference in signal compared to the vehicle-treated control (Figure 3c,d). We also found that bisulfite addition alone does not yield a discernable response from the vehicle control. These experiments further support the ability of **CFAP700** to detect changes in FA levels in living mice.

Finally, we demonstrated that the **CFAP700** probe can detect endogenous FA fluxes that are produced by the folate cycle, particularly through tetrahydrofolate metabolism (Figure 4). In these experiments, mice were injected with either vehicle (DMSO) or tetrahydrofolate (30 mpk), vehicle (water) or sodium bisulfite (25 mpk), and then 100 μM **CFAP700**. We observed an immediate difference at the first imaging point between the tetrahydrofolate- and vehicle-treated mice, which is consistent with the rapid rate of tetrahydrofolate metabolism detailed recently in cell models.[8]

In separate control experiments, we did not find any statistically significant differences between vehicle-treated

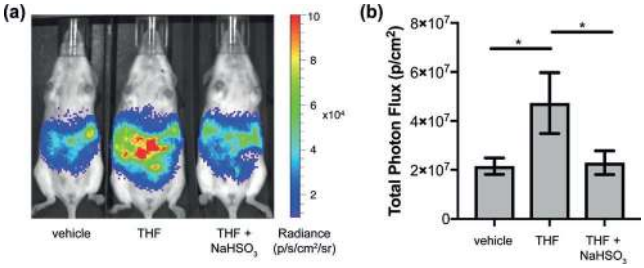

Figure 4. FVB-luc+ mice were injected (i.p.) with tetrahydrofolate (30 mpk) or DMSO, then aq. sodium bisulfite (25 mpk) or water, then 100 μM **CFAP700** (100 μL, 1% DMSO, 1% BSA in PBS). The mice were imaged every 2.5 min from 0–25 min. a) Representative images of FVB-luc+ mice injected with **CFAP700**, tetrahydrofolate, and/or bisulfite. b) Total photon flux, integrated from 0–25 min post injection. Error bars = SEM ($n = 4$–5). Statistical analyses were performed with a two-tailed Student's t test where $^*P \leq 0.05$.

mice and tetrahydrofolate-treated mice that were also exposed to the FA scavenger sodium bisulfite (25 mpk), which further establishes that the increased emission signal we observe upon tetrahydrofolate injection arises from the generation of FA from endogenous folate metabolism. Interestingly, we show that treatment with an equimolar quantity of aqueous calcium folinate (37 mpk) followed by **CFAP700** injection does not give any discernable difference in chemiluminescent signal over that of vehicle-treated mice (Supporting Information, Figure S7). These data reveal that folinate and tetrahydrofolate, two important components of the folate cycle, show starkly different metabolic activities related to FA where folinate does not produce FA[49] and tetrahydrofolate is an effective FA producer in vivo.

In conclusion, we have reported a first-generation pair of chemiluminescent probes for FA utilizing a general 2-aza-Cope FA-reactive trigger and a chemiluminogenic phenoxy-dioxetane scaffold. Functionalization at the *ortho*-position of the phenol yielded two distinct reagents that span the ability to monitor FA from in vitro biochemical to cell to in vivo animal models. Both **CFAP540** and **CFAP700** show high selectivity and sensitivity to FA; the cell-trappability of **CFAP540** makes it suitable for cellular FA detection whereas the red-shifted emission profile of **CFAP700** can be exploited for live-animal FA visualization. Moreover, **CFAP700** provides the first in vivo evidence that folinate and tetrahydrofolate have distinct abilities to generate FA through folate cycle metabolism, presaging the utility of the CFAP platform and related chemical tools to help disentangle the complex pathways of FA production, metabolism, and signaling, particularly in the context of one-carbon biological chemistry. Finally, this work provides a general path forward to develop bright and tunable chemiluminescent ABS probes for a broader range of biological analytes that can be used in various types of specimens.

Acknowledgements

This work was supported by the NIH (NIEHS 28096 and NIEHS 04705 to C.J.C.). K.J.B. was partially supported by an NSF graduate fellowship. T.A.S. was supported by an NIH Ruth L. Kirschstein NRSA Fellowship (F32 GM122248). C.J.C. is an Investigator of the Howard Hughes Medical Institute. We thank Prof. Marie Heffern, Ms. Diyala Shihadih, and Prof. Andreas Stahl for providing us with initial breeding pairs for our in-house breeding colony.

Conflict of interest

The authors declare no conflict of interest.

Keywords: activity-based sensing · chemiluminescence · formaldehyde · one-carbon metabolism · oxetane

How to cite: *Angew. Chem. Int. Ed.* **2018**, *57*, 7508–7512
Angew. Chem. **2018**, *130*, 7630–7634

[1] R. Q. He, J. Lu, J. Y. Miao, *Sci. China Life Sci.* **2010**, *53*, 1399–1404.
[2] R. G. Liteplo, R. Beauchamp, M. E. Meek, R. Chénier, *Formaldehyde: Concise International Chemical Assessment Document 40*, **2002**.
[3] A. S. Tibbetts, D. R. Appling, *Annu. Rev. Nutr.* **2010**, *30*, 57–81.
[4] J. W. Locasale, *Nat. Rev. Cancer* **2013**, *13*, 572–583.
[5] P. M. Tedeschi, E. K. Markert, M. Gounder, H. Lin, D. Dvorzhinski, S. C. Dolfi, L. L. Y. Chan, J. Qiu, R. S. DiPaola, K. M. Hirshfield, et al., *Cell Death Dis.* **2013**, *4*, e877.
[6] M. Ehrlich, *Oncogene* **2002**, *21*, 5400–5413.
[7] S. C. Lu, J. M. Mato, *Physiol. Rev.* **2012**, *92*, 1515–1542.
[8] G. Burgos-Barragan, N. Wit, J. Meiser, F. A. Dingler, M. Pietzke, L. Mulderrig, L. B. Pontel, I. V. Rosado, T. F. Brewer, R. L. Cordell, et al., *Nature* **2017**, *548*, 549–554.
[9] S. Hamm, G. Just, N. Lacoste, N. Moitessier, M. Szyf, O. Mamer, *Bioorg. Med. Chem. Lett.* **2008**, *18*, 1046–1049.
[10] L. J. Walport, R. J. Hopkinson, C. J. Schofield, *Curr. Opin. Chem. Biol.* **2012**, *16*, 525–534.
[11] J. Chan, S. C. Dodani, C. J. Chang, *Nat. Chem.* **2012**, *4*, 973–984.
[12] M. H. Lee, J. S. Kim, J. L. Sessler, *Chem. Soc. Rev.* **2015**, *44*, 4185–4191.
[13] X. Chen, X. Tian, I. Shin, J. Yoon, *Chem. Soc. Rev.* **2011**, *40*, 4783.
[14] Y. Yang, Q. Zhao, W. Feng, F. Li, *Chem. Rev.* **2013**, *113*, 192–270.
[15] K. J. Bruemmer, T. F. Brewer, C. J. Chang, *Curr. Opin. Chem. Biol.* **2017**, *39*, 17–23.
[16] Z. Xu, J. Chen, L.-L. Hu, Y. Tan, S.-H. Liu, J. Yin, *Chin. Chem. Lett.* **2017**, *28*, 1935–1942.
[17] T. F. Brewer, C. J. Chang, *J. Am. Chem. Soc.* **2015**, *137*, 10886–10889.
[18] A. Roth, H. Li, C. Anorma, J. Chan, T. F. Brewer, C. J. Chang, A. Roth, H. Li, C. Anorma, J. Chan, *J. Am. Chem. Soc.* **2015**, *137*, 10890–10893.
[19] W. Liu, C. Truillet, R. R. Flavell, T. F. Brewer, M. J. Evans, D. M. Wilson, C. J. Chang, *Chem. Sci.* **2016**, *7*, 5503–5507.
[20] K. J. Bruemmer, R. R. Walvoord, T. F. Brewer, G. Burgos-Barragan, N. Wit, L. B. Pontel, K. J. Patel, C. J. Chang, *J. Am. Chem. Soc.* **2017**, *139*, 5338–5350.
[21] T. F. Brewer, G. Burgos-Barragan, N. Wit, K. J. Patel, C. J. Chang, *Chem. Sci.* **2017**, *8*, 4073–4081.
[22] K. Dou, G. Chen, F. Yu, Y. Liu, L. Chen, Z. Cao, T. Chen, Y. Li, J. You, *Chem. Sci.* **2017**, *8*, 7851–7861.
[23] Y. Zhou, J. Yan, N. Zhang, D. Li, S. Xiao, K. Zheng, *Sens. Actuators B* **2018**, *258*, 156–162.
[24] X. Xie, F. Tang, X. Shangguan, S. Che, J. Niu, Y. Xiao, X. Wang, B. Tang, *Chem. Commun.* **2017**, *53*, 6520–6523.
[25] C. Liu, X. Jiao, S. He, L. Zhao, X. Zeng, *Dye. Pigment.* **2017**, *138*, 23–29.
[26] L. He, X. Yang, M. Ren, X. Kong, Y. Liu, W. Lin, *Chem. Commun.* **2016**, *52*, 9582–9585.
[27] Z. Xie, J. Ge, H. Zhang, T. Bai, S. He, J. Ling, H. Sun, Q. Zhu, *Sens. Actuators B* **2017**, *241*, 1050–1056.
[28] Y. Tang, X. Kong, A. Xu, B. Dong, W. Lin, *Angew. Chem. Int. Ed.* **2016**, *55*, 3356–3359; *Angew. Chem.* **2016**, *128*, 3417–3420.
[29] F. Wu, Y. Zhang, L. Huang, D. Xu, H. Wang, *Anal. Methods* **2017**, *9*, 5472–5477.
[30] Y. H. Lee, Y. Tang, P. Verwilst, W. Lin, J. S. Kim, *Chem. Commun.* **2016**, *52*, 11247–11250.
[31] Y. Tang, X. Kong, Z.-R. Liu, A. Xu, W. Lin, *Anal. Chem.* **2016**, *88*, 9359–9363.
[32] X. Song, X. Han, F. Yu, J. Zhang, L. Chen, C. Lv, *Analyst* **2018**, *143*, 429–439.
[33] A. R. Lippert, *ACS Cent. Sci.* **2017**, *3*, 269–271.
[34] N. Hananya, D. Shabat, *Angew. Chem. Int. Ed.* **2017**, *56*, 16454–16463; *Angew. Chem.* **2017**, *129*, 16674–16683.
[35] C. Dodeigne, L. Thunus, R. Lejeune, *Talanta* **2000**, *51*, 415–439.

[36] S. Gnaim, O. Green, D. Shabat, *Chem. Commun.* **2018**, *54*, 2073 – 2085.
[37] X. Li, X. Gao, W. Shi, H. Ma, *Chem. Rev.* **2014**, *114*, 590 – 659.
[38] A. P. Schaap, T. Chen, R. S. Handley, *Tetrahedron Lett.* **1987**, *28*, 1155 – 1158.
[39] M. C. Thurnauer, M. K. Bowman, B. T. Cope, J. R. Norris, *J. Am. Chem. Soc.* **1978**, *100*, 1965 – 1966.
[40] N. Hananya, O. Green, R. Blau, R. Satchi-Fainaro, D. Shabat, *Angew. Chem. Int. Ed.* **2017**, *56*, 11793 – 11796; *Angew. Chem.* **2017**, *129*, 11955 – 11958.
[41] J. Cao, R. Lopez, J. M. Thacker, J. Y. Moon, C. Jiang, S. N. S. Morris, J. H. Bauer, P. Tao, R. P. Mason, A. R. Lippert, *Chem. Sci.* **2015**, *6*, 1979 – 1985.
[42] O. Green, T. Eilon, N. Hananya, S. Gutkin, C. R. Bauer, D. Shabat, *ACS Cent. Sci.* **2017**, *3*, 349 – 358.
[43] J. Cao, W. An, A. G. Reeves, A. R. Lippert, *Chem. Sci.* **2018**, *9*, 2552 – 2558.
[44] S. Sun, Z. Bao, H. Ma, D. Zhang, X. Zheng, *Biochemistry* **2007**, *46*, 6668 – 6673.
[45] M. E. Roth-Konforti, C. R. Bauer, D. Shabat, *Angew. Chem. Int. Ed.* **2017**, *56*, 15633 – 15638; *Angew. Chem.* **2017**, *129*, 15839 – 15844.
[46] J. Cao, J. Campbell, L. Liu, R. P. Mason, A. R. Lippert, *Anal. Chem.* **2016**, *88*, 4995 – 5002.
[47] O. Green, S. Gnaim, R. Blau, A. Eldar-Boock, R. Satchi-Fainaro, D. Shabat, *J. Am. Chem. Soc.* **2017**, *139*, 13243 – 13248.
[48] A. Duong, C. Steinmaus, C. M. McHale, C. P. Vaughan, L. Zhang, *Mutat. Res. Rev. Mutat. Res.* **2011**, *728*, 118 – 138.
[49] F. Scaglione, G. Panzavolta, *Xenobiotica* **2014**, *44*, 480 – 488.

Manuscript received: February 16, 2018
Accepted manuscript online: April 10, 2018
Version of record online: April 27, 2018

